Available online at BCREC website: https://bcrec.id

Bulletin of Chemical Reaction Engineering & Catalysis, 18 (3) 2023, 375-385

Research Article

Synthesis of ZnO Nanoparticle using Lidah Mertua (*Sansevieria trifasciata*) Extract through Sol-Gel Method and Its Application for Methylene Blue Photodegradation

Nanda Saridewi[1,*], Selviana Rustanti[2], Agustino Zulys[3], Siti Nurbayti[2], Isalmi Aziz[2], Adawiah Adawiah[4]

[1]*Department of Chemistry Education, Faculty of Tarbiya and Teaching Science UIN Syarif Hidayatullah Jakarta, Jl. Ir. H. Juanda No. 95 Ciputat, Tangerang Selatan 15412, Indonesia.*
[2]*Department of Chemistry, Faculty of Science and Technology, UIN Syarif Hidayatullah Jakarta, Jl. Ir. H. Juanda No. 95 Ciputat, Tangerang Selatan 15412, Indonesia.*
[3]*Department of Chemistry, Faculty of Mathematics and Natural Sciences, University of Indonesia, Jl. Lingkar Kampus Raya, Pondok Cina, Beji, Depok, Jawa Barat 16424, Indonesia.*
[4]*Integrated Laboratory Centre, Faculty of Science and Technology UIN Syarif Hidayatullah Jakarta, Jl. Ir. H. Juanda No. 95 Ciputat, Tangerang Selatan 15412, Indonesia.*

Received: 25th July 2023; Revised: 17th August 2023; Accepted: 17th August 2023
Available online: 25th August 2023; Published regularly: October 2023

Abstract

Methylene blue is widely used in the textile industry and is difficult to degrade naturally because of its heterocyclic aromatic structure. One technique that can be used to degrade methylene blue is through a photocatalytic process using ZnO nanoparticles. This study aims to synthesize ZnO nanoparticles using *Lidah mertua* extract (*Sansevieria trifasciata*) as a capping agent by the sol-gel method, and determine the characteristics and stability of ZnO nanoparticles in methylene blue photodegradation. The synthesis of ZnO nanoparticles begins with drying *Lidah mertua*, grinding it, and then extracting it using distilled water. Furthermore, the extract was reacted with $Zn(CH_3COO)_2.2H_2O$ 0.15 M at pH 8. The extract was characterized using Fourier Transform Infrared (FTIR), and the ZnO nanoparticles were characterized using X-Ray Diffraction (XRD), ultraviolet-visible (UV-Vis) DRS, and Scanning Electron Microscopy (SEM). *Lidah mertua* extract has OH (hydroxyl), CN, CH, and C=C functional groups. The obtained ZnO nanoparticles have a crystal size of 19.324 nm. The crystalline phase is hexagonal; the morphology is spherical, with a particle size of 79.153 nm and a band gap energy of 3.21 eV. ZnO nanoparticles exhibited a methylene blue decolorization of 98.50% through 43.41% by adsorption and 55.09% by photocatalytic mechanism. ZnO nanoparticles showed good stability for a three-cycle reaction.

Copyright © 2023 by Authors, Published by BCREC Group. This is an open access article under the CC BY-SA License (https://creativecommons.org/licenses/by-sa/4.0).

Keywords: Methylene blue; photocatalyst; *Sansevieria trifasciata*; ZnO nanoparticles

How to Cite: N. Saridewi, S. Rustanti, A. Zulys, S. Nurbayti, I. Aziz, A. Adawiah (2023). Synthesis of ZnO Nanoparticle using Lidah Mertua (*Sansevieria trifasciata*) Extract through Sol-Gel Method and Its Application for Methylene Blue Photodegradation. *Bulletin of Chemical Reaction Engineering & Catalysis*, 18(3), 375-385 (doi: 10.9767/bcrec.19647)

Permalink/DOI: https://doi.org/10.9767/bcrec.19647

1. Introduction

Methylene blue is widely used in the textile industry because it can stick strongly to cotton and cloth fibers [1]. Methylene blue is a dye with a heterocyclic aromatic structure that is difficult to degrade in nature [2]. Methylene blue releases harm the environmental ecosystem and cause cyanosis, vomiting, increased heart rate, and tissue necrosis in humans [3,4].

* Corresponding Author.
Email: nanda.saridewi@uinjkt.ac.id (N. Saridewi);
Telp: +62 852-6302-0374

Photocatalytic process is considered the efficient method can be employed to minimize methylene blue pollution. The photocatalytic process combines a catalytic and photochemical processes. Photocatalytic involves light, which functions as a trigger and catalyst to accelerate the transformation process. This method can react quickly with various dyes in water due to the formation of hydroxyl (•OH) radicals, low operating costs, and high reusability [5,6]. The degradation of dye pollutants by the photocatalyst process usually uses a semiconductor-based ZnO nanoparticles [7,8].

ZnO nanoparticles can be synthesized using various methods, such as hydrothermal, sol-gel, precipitation, sonochemical, and microemulsion methods [9]. The sol-gel method is widely used to synthesize ZnO nanoparticles because it utilizes a low temperature, the consequent product with good homogeneity, more rapid crystal formation, and quite low waste [10]. However, the sol-gel method requires capping agents derived from chemicals like CTAB (Cetyl Trimethyl Ammonium Bromide), TEA (Triethanolamine), and HMTA (Hexamethylene Tetramine) that are not environmentally friendly [11].

In recent years, many researchers have developed the green synthesis method to construct ZnO nanoparticles to reduce the usage of hazardous chemicals. This green synthesis method employs a natural capping agent derived from plant extracts [12]. One plant extract that has the potential as a capping agent in the synthesis of ZnO nanoparticles is *Lidah mertua* plant. *Lidah Mertua* extract contains flavonoids, tannins, and phenols, which serve as capping agents to prevent agglomeration in the synthesis of nanoparticles [13].

Based on our knowledge, the synthesis of ZnO nanoparticles using *Lidah mertua* extract as a capping agent has never been carried out. Therefore, this study employs the sol-gel method to synthesize ZnO nanoparticles using *Lidah mertua* extract as a capping agent. The ZnO nanoparticles were then characterized using a UV-VIS DRS spectrophotometer, X-Ray Diffraction (XRD), and Scanning Electron Microscope (SEM). The ZnO nanoparticles' photocatalytic activity was analyzed for the degradation of methylene blue under a 250-watt mercury lamp irradiation. The test was optimized by experimenting with variations, namely the mass of ZnO nanoparticles, the concentration of methylene blue, and the pH of the solution. The addition of electron-hole scavengers in the form of H_2O_2, CH_3OH, and tertiary butanol was also carried out to determine which species had a dominant role in the degradation process. The stability test of nanoparticles was carried out by repeating the photocatalytic degradation reaction of methylene blue for 3 reaction cycles.

2. Materials and Methods

2.1 Materials

The materials were used without any purification, included dried *Lidah mertua* (*Sansevieria trifasciata*), zinc acetate dihydrate ($Zn(CH_3COO)_2.2H_2O$) (Merck, p.a.), NaOH (Merck, p.a.), H_2O_2 (Merck, p.a.), CH_3OH (Merck, p.a.), tert-butanol (Merck, p.a.), methylene blue (Merck, p.a.), and distilled water.

2.2 *Lidah Mertua* Extraction

As much as 10 g of dried *Sansevieria trifasciata* powder is placed in a beaker, and 100 mL of distilled water is added. Furthermore, the mixture was stirred using a magnetic stirrer at 400 rpm while heated in a water bath at 100 °C for 25 min. The mixture was filtered, and the extract was analyzed using FTIR to determine the functional groups and active compounds contained in the extract.

2.3 Determination of Total Flavonoid of *Lidah Mertua* Extract

1 mL of *Lidah mertua* extract with a concentration of 1 mg/mL was added to a mixture of 1 mL of 2% $AlCl_3$ solution and 1 mL of 120 mM potassium acetate. The mixture was incubated at room temperature for 1 h. The absorbance of the mixture was measured using a UV-Vis spectrophotometer at 435 nm. Quercetin solution was used as a standard solution of flavonoids.

2.4 Synthesis of ZnO Nanoparticles

10 mL of *Sansevieria trifasciata* extract was reacted with 90 mL of 0.15 M $Zn(CH_3COO)_2.2H_2O$. Then, the mixture was stirred using a magnetic stirrer at 400 rpm while heated at 70 °C for 1 h. The NaOH solution was then added to the mixture gradually until the pH of the mixture was 8. The resulting yellowish-white solid was then centrifuged at 4000 rpm. Solids were taken and washed using distilled water and dried at 100 °C for 18 h. The solid was then calcined at 450 °C for 4 h to obtain ZnO nanoparticles powder.

2.5 Characterization of ZnO Nanoparticles

The resulting ZnO nanoparticles were characterized using XRD to determine their diffrac-

Copyright © 2023, ISSN 1978-2993

tion patterns using monochromatic Cu-Kα radiation (λ = 1.54056 Å). Crystallinity, and phase type were determined by processing the XRD test diffractogram data using the Match 3.0 application. Spectrophotometer UV-Vis DRS is used to measure the band gap energy value. The Tauc-Plot and Kubelka Munk formula was employed to determine the band gap energy [14]. ZnO nanoparticles were also analyzed for morphology using a scanning electron microscope (SEM) JEOL JSM-6510LA.

2.5 Photocatalytic Activity of ZnO Nanoparticles

The ZnO nanoparticles were dispersed into 100 mL of methylene blue solution, stirred using a magnetic stirrer at 300 rpm at room temperature, and irradiated with a 250-watt mercury lamp for 2 h. The suspension was sampled at 2 mL every 10 min and centrifuged at 6000 rpm for 10 min. The absorbance of methylene blue was measured using a UV-Vis spectrophotometer at a wavelength of 665. The efficiency of dye degradation was calculated using equation (1).

$$DE(\%) = \frac{A_0 - A_t}{A_0} \times 100\% \quad (1)$$

where, DE is degradation efficiency of methylene blue (%), A_0 is the initial absorbance of methylene blue and A_t is the absorbance of methylene blue at time.

Optimization of the photodegradation of methylene blue by ZnO nanoparticles was carried out using a variety of methylene blue concentrations (20; 25; and 30 ppm), the mass of ZnO nanoparticles (75, 100, and 125 mg), the pH of the solution (pH = 5, 7, and 9), and the measurement of the effect of the addition of H_2O_2, CH_3OH, and tert-butanol to determine which species plays a dominant role in the photocatalytic degradation process of methylene blue.

2.6 Reusability and Stability Test of ZnO Nanoparticles

The reusability test of ZnO nanoparticles was carried out by measuring the degradation efficiency of methylene blue with three cycles reaction. This test was carried out with the photocatalyst's mass, the initial methylene blue's concentration, and the pH at the optimum conditions. After the reaction, the ZnO photocatalyst was separated, dried, and analyzed using XRD to determine its stability.

3. Results and Discussion

3.1 Total Flavonoid Content of *Sansevieria trifasciata* Extract

The *Sansevieria trifasciata* extract showed a total flavonoid content of 0.43 mg/g QE (quercetin equivalent). Therefore, the extract of *Sansevieria trifasciata* can be utilized as a capping agent in the synthesis of ZnO nanoparticles. It is supported by previous studies using *Punica granatum* extract with a total flavonoid content of 0.459 mg/g, which was used as a capping agent to synthesize ZnO nanoparticles [15]. Marslin *et al.* [16] stated that flavonoids play the most roles as both capping and reducing agents in the green synthesis of nanoparticles. It is due to the hydroxyl groups in flavonoid structure have a negative charge that can be covered by negatively charged ions resulting in repulsive forces between like charges; this

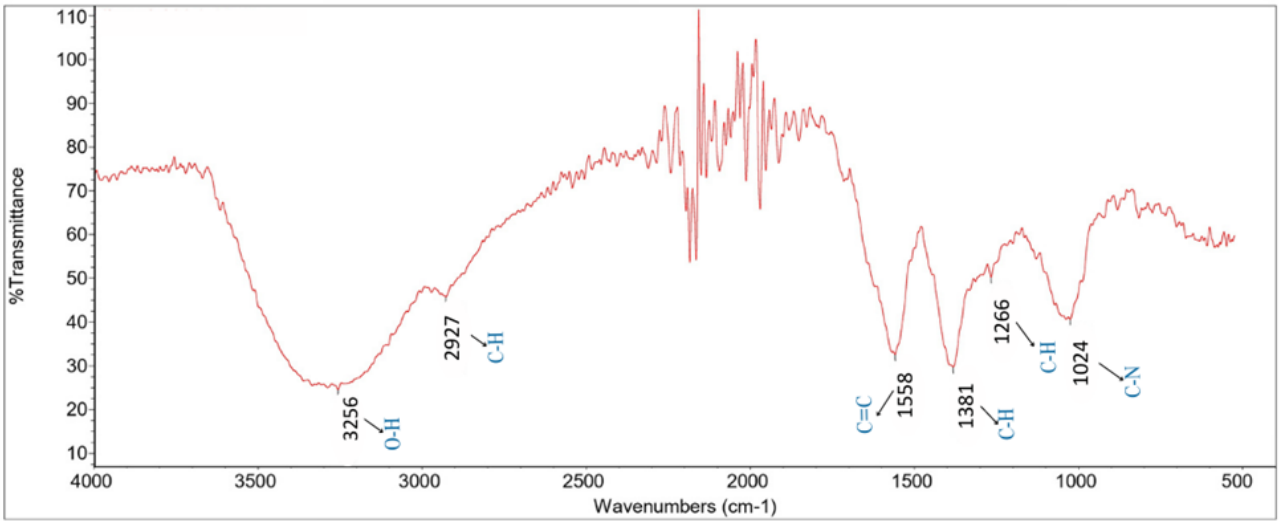

Figure 1. FTIR spectrum of *Sansevieria trifasciata* extract.

Copyright © 2023, ISSN 1978-2993

prevents aggregation between ZnO nanoparticles [17].

Figure 1 shows the presence peak at 3256 cm^{-1}, characteristic of the OH vibration, indicating the presence of phenolic hydroxyl groups. Absorption peaks at 3200–3310 cm^{-1} indicate the presence of the OH functional group in polyphenols, proteins / enzymes, or polysaccharides / carbohydrates. Absorption peak at 2927 cm^{-1}, indicating the presence of the CH stretching polyol functional group. A peak at 1558 cm^{-1} indicates the presence of the functional group C=C in the aromatic ring. The peak at 1381 cm^{-1} indicates the presence of amine-bending CH vibrations. The peak at 1265 cm^{-1} indicates the presence of a CH stretching amine vibration. The peak at 1024 cm^{-1} indicates the presence of the CN functional group in the extract [18]. Based on the FTIR results, it is known that *Sansevieria trifasciata* extract contains functional groups of flavonoid compounds, polyols, and also proteins that can play a role in the process of reducing Zn^{2+} to ZnO. Nurbayasari *et al.* [19] stated that the flavonoids, polyols, and proteins that have functional groups, such as alcohols, carboxylic acids, and amines play an important role during the reduction process in the synthesis of ZnO nanoparticles.

3.2 ZnO Nanoparticles

The formation of ZnO nanoparticles using the sol-gel method occurs when the $Zn(CH_3COO)_2.2H_2O$ and *Sansevieria trifasciata* extract react. *Sansevieria trifasciata* acts as a capping and reducing agent. Meanwhile, NaOH acts as a reducing agent. The precursor concentration used in this reaction is 0.15 M at pH 8. It is because the concentration of 0.15 M and pH 8 is the best conditions for the biosynthesis of ZnO nanoparticles [19]. pH 8 is a stable condition in synthesizing ZnO nanoparticles because, at a pH less than 8, there is aggregation on the surface of ZnO particles, which causes the ZnO particle size to become more extensive [11]. The overall mechanism for creating the ZnO nanoparticle can be seen in Figure 2.

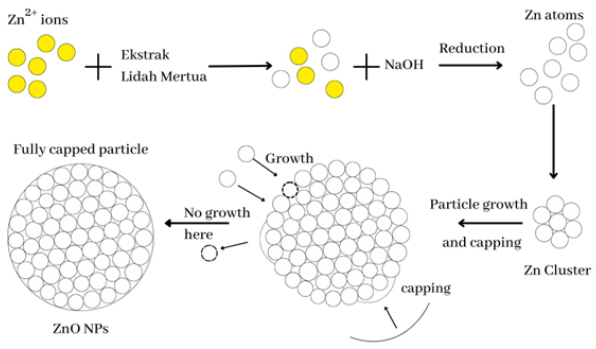

Figure 2. Synthesis mechanism of ZnO nanoparticles [19].

The functional groups derived from *Sansevieria trifasciata* extract and NaOH reduce Zn^{2+} to Zn. Therefore, the Zn atoms form and combine to form Zn clusters. The functional group derived from *Sansevieria trifasciata* extract interacts with the Zn surface to enfold the Zn clusters and form a capping. This capping prevents aggregation between Zn clusters to form stable ZnO nanoparticles. The negatively charged hydroxyl groups derived from *Sansevieria trifasciata* extract can surround the surface of the particles resulting in repulsive forces between like charges. It prevents aggregation between ZnO nanoparticles [17].

In addition, the functional groups in *Sansevieria trifasciata* extract undergo a complexation reaction with Zn^{2+}. The functional groups in *Sansevieria trifasciata* extract roles as a ligand and Zn^{2+} acts as a metal in this complexation reaction [11]. The functional groups in *Sansevieria trifasciata* extract donate free electron pairs to Zn^{2+} metal ions to form nano-sized complex compounds, and ZnO nanoparticles are formed after the calcination process [20].

3.3 Crystallinity of ZnO Nanoparticles

ZnO nanoparticles were characterized using X-Ray Diffraction to determine the crystallinity and diffraction pattern formed. The X-Ray Diffraction data obtained were processed using Origin and Match software as reference databases for crystal phases and ZnO peaks. The results of the X-Ray Diffraction ZnO characterization are presented in Figure 3.

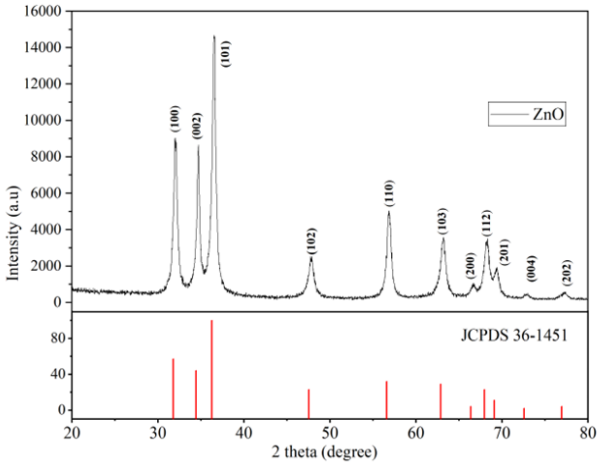

Figure 3. XRD spectrum of ZnO Nanoparticles.

Copyright © 2023, ISSN 1978-2993

Figure 3 shows that the resulting ZnO has a hexagonal wurtzite-shaped crystalline phase and good crystallinity as seen from the high intensity of the diffraction peak at 2θ, which is 32.018°; 34.669°; 36.555°; 47.798°; 56.801°; 63.078°; 66.79°; 68.219°; 69.343°; 72.79°; and 77.35° with *hkl* index of (100), (002), (101), (102), (110), (103), (200), (112), (201), (004), and (202) (JCPDS ZnO No. 36-1451).

3.4 Band Gap Energy of ZnO Nanoparticles

The band gap energy's value is determined using the Kubelka-Munk equation combined with the Tauc plot. The results of the band gap energy of ZnO nanoparticles can be seen in Figure 4. The Figure 4 shows that ZnO nanoparticles have a band gap energy of 3.21 eV, and maximum light absorption occurs at 400 nm, so that the synthesized ZnO can be used as a photocatalyst under UV light irradiation.

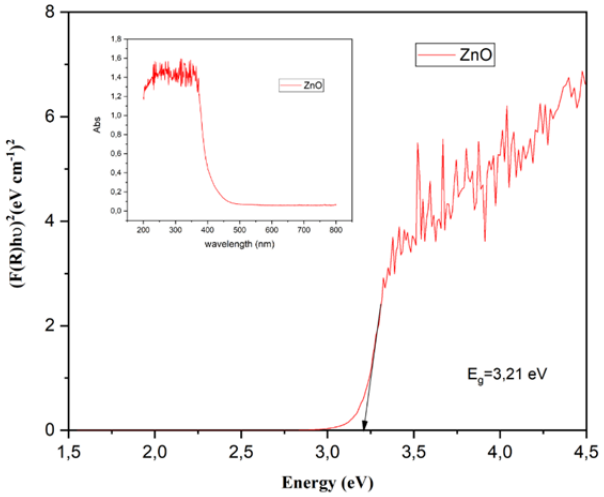

Figure 4. Band gap energy of ZnO nanoparticles.

3.5 ZnO Nanoparticle Morphology

The morphology of ZnO nanoparticles using SEM can be seen in Figure 5. The ZnO nanoparticle size was calculated using Image J software. The Figure 5(a) shows that ZnO nanoparticles have a spherical morphology with gaps between the particles that cannot be seen clearly. It is due to agglomeration between ZnO particles [21]. Agglomeration can be driven by several things, like the influence of polarity, ZnO electrostatic forces, and the large energy on the sample's surface that occurs during the synthesis process. The agglomeration of ZnO is thought to be due to *Lidah mertua* extract which contains many chemical compounds so that the compound acts as a trap or template for the precursor $Zn(CH_3COO)_2.2H_2O$. Sari *et al.* [12] explained that the size of the template surrounding the surface of the nanoparticles also greatly influences the size of the resulting ZnO nanoparticles. The obtained ZnO nanoparticles in this study have various diameter sizes. Figure 5(b) shows the 40–140 nm particle size distribution with an average diameter of 79.1532 nm. Vasquez *et al.* [22] state that particles with a diameter of <1,000 nm can still be considered as nanoparticles.

3.6 Photocatalytic Activity of ZnO Nanoparticles

The dark test was carried out to know the adsorption ability of ZnO nanoparticles in degrading methylene blue. Figure 6 shows that ZnO nanoparticles could degrade methylene blue via two mechanisms, the adsorption and the photocatalytic mechanism. The degradation efficiency of methylene blue in the dark

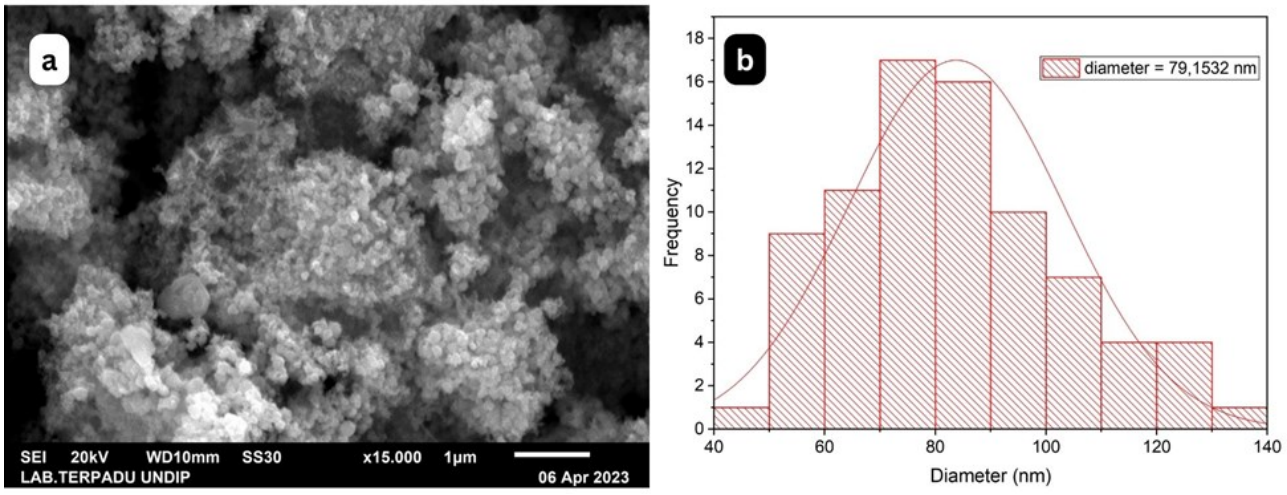

Figure 5. ZnO nanoparticle morphology (a) with 15000x magnification and (b) ZnO particle diameter distribution.

Copyright © 2023, ISSN 1978-2993

condition was 43.41%. It indicated that ZnO nanoparticles could adsorb methylene blue.

Meanwhile, the degradation efficiency of methylene blue in light condition was greater than in dark conditions, which was 98.50%. Therefore, the degradation of methylene blue through the photocatalytic pathway was 55.09%. In light conditions, when ZnO was irradiation by UV light from a mercury lamp, the electron excitation from the valence band to the conduction band was ensued and produces an electron hole (h^+) in the valence band (equation (2)). The electron holes then absorb water molecules and produce hydroxyl radicals (•OH) (equation (3)). At the same time, the excited electrons in the conduction band react with oxygen to form superoxide radicals ($•O_2$) (equation (4)). Superoxide radicals ($•O_2$) react with adsorbed water to produce hydroxide ions which react with electron holes to form hydroxyl radicals (•OH), which are strong oxidizing agents (equations (5) and (6)). Furthermore, methylene blue is oxidized by hydroxyl radicals (•OH) to produce carbon dioxide and water [23].

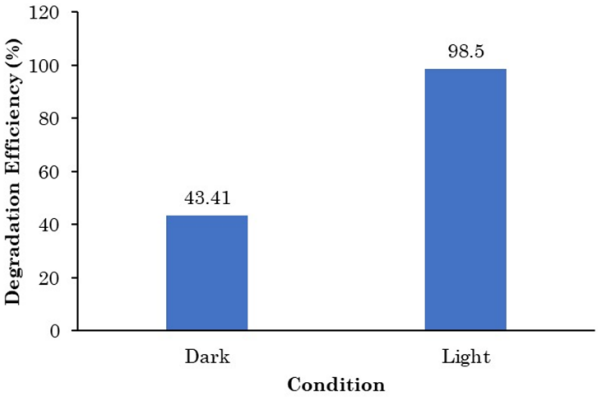

Figure 6. The efficiency degradation of methylene blue by ZnO nanoparticles in dark and light condition.

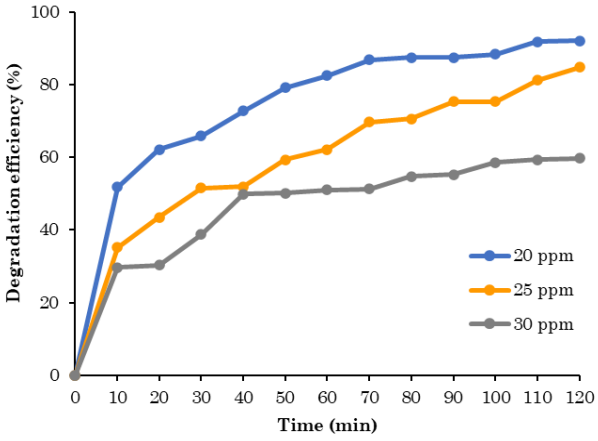

Figure 7. Effect of initial methylene blue concentration on methylene blue degradation efficiency.

$$ZnO + h\upsilon \rightarrow ZnO\ (e^-_{cb} + h^+_{vb}) \quad (2)$$

$$H_2O + h^+_{vb} \rightarrow •OH + H^+ \quad (3)$$

$$O_2 + e^-_{cb} \rightarrow •O_2 \quad (4)$$

$$h^+_{vb} + OH^- \rightarrow •OH \quad (5)$$

$$OH + \text{MB dyes} \rightarrow \text{degraded product} + CO_2 + H_2O \quad (6)$$

3.7 Effect of Methylene Blue Concentration

The effect of initial methylene blue concentration to degradation efficiency can be seen in Figure 7. The Figure 7 shows the highest degradation efficiency is at methylene blue 20 ppm with a degradation efficiency of 92.05%. A methylene blue concentration of 30 ppm decreased degradation efficiency. It is because the photocatalyst is already in a saturated phase due to the high concentration of methylene blue covering the photocatalyst surface, causing a decrease in photon efficiency and deactivation of the photocatalys. Balcha *et al.* [24] explained that the degradation of dyes would decrease as the concentration of the dyes increased due to the high concentration of dyes reducing the intensity of photons hitting the surface of the photocatalyst due to photon absorption by the dye molecules in the system.

3.8 Effect of ZnO Dosage

The effect of ZnO dosage to degradation efficiency can be seen in Figure 8. The Figure 8 shows that the use of a ZnO dosage of 75 mg resulted in a degradation efficiency of 82.92%. It is greater than ZnO dosage of 100 mg and 125 mg. It was because the turbidity of the solution increased due to the number of ZnO particles increased. The turbidity blocks UV

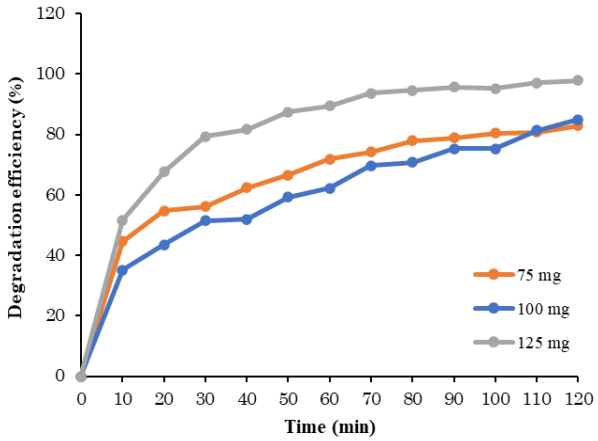

Figure 8. Effect of ZnO dosage on degradation efficiency of methylene blue.

Copyright © 2023, ISSN 1978-2993

radiation, thereby preventing the penetration of light into the solution, resulting in the inhibition of the formation of excited electrons, which play a role in the degradation process of the dye, causing a decrease in photocatalytic activity. It indicates that adding an excess amount of photocatalyst or exceeding the optimum limit is ineffective in forming hydroxyl radicals and superoxides [25–27].

3.9 Effect of pH

This test was carried out in 3 conditions, namely acidic, neutral and alkaline with the aim of determining the stability and also the optimum photocatalytic activity of ZnO (Figure 9). The acidic conditions at pH 5 resulted in a mere small degradation efficiency of 23.26%, so it is known that ZnO does not have photocatalytic activity. It is because at low pH, the H^+ ion is the prevalent species, so the positively charged ZnO interacts more with H^+ ions that compete with the positive charge on methylene blue, so this reaction is less favored and causes a decrease in methylene blue degradation [27,28]. The degradation efficiency at pH 7 and 9 was higher than at pH 5. At pH 9 or alkaline conditions, the degradation efficiency was 98.50%. It indicates more optimum degradation obtained under alkaline (pH 9) than acidic conditions. During alkaline conditions, the surface charge of ZnO is more negatively charged so that positively charged methylene blue interact with the surface of ZnO, which tends to be negatively charged (equations (7) and (8)).

In addition, the effectiveness of degradation increases at alkaline pH because an increase in the amount of OH^- leads to an increase in the amount of $OH\bullet$ radicals produced. The more OH radicals formed, the greater the degradation efficiency of the methylene blue [28].

$$(pH < 6.8) : Zn{-}OH + H^+ \rightarrow ZnOH^{2+} \quad (7)$$
$$(pH > 6.8) : Zn{-}OH + OH^- \rightarrow ZnO^- + H_2O \quad (8)$$

3.10 Effect of Sacrificial Agent

The addition of H_2O_2 in this test was used as an excited electron-capturing agent (e^-), tertiary butanol as a hydroxyl radical scavenging agent ($\bullet OH$), and methanol was used as an electron-hole capturing agent (h^+). Figure 10 shows the photocatalytic activity of ZnO with the addition of hydrogen peroxide (H_2O_2) is higher than methanol and a mixture of Tert-BuOH and H_2O_2, which results in a degradation efficiency of 75.36%. Meanwhile, adding methanol and a mixture of H_2O_2 and tert-BuOH resulted in a degradation efficiency of 52.67% and 61.50%, respectively.

Adding H_2O_2 as an electron-capturing agent prevents recombination between excited electrons and electron holes. The excited electrons are captured by H_2O_2 and cause a decrease in the recombination rate resulting in inhibition of recombination between electrons and electron holes. Thus the addition of H_2O_2 can increase the photocatalytic activity of ZnO. H_2O_2 reacts with the excited electrons to produce hydroxide ions (OH^-) and hydroxyl radicals ($\bullet OH$) (equations (9) and (11)). On the other hand, the added H_2O_2 is decomposed by light to produce hydroxyl radicals. It causes an increase in the number of hydroxyl radical species increasing the efficiency of methylene blue degradation [29].

$$e^-_{cb} + H_2O_2 \rightarrow \bullet OH + OH^- \quad (9)$$
$$H_2O_2 + Light \rightarrow \bullet OH + OH^- \quad (10)$$
$$h^+_{vb} + H_2O \rightarrow \bullet OH \quad (11)$$

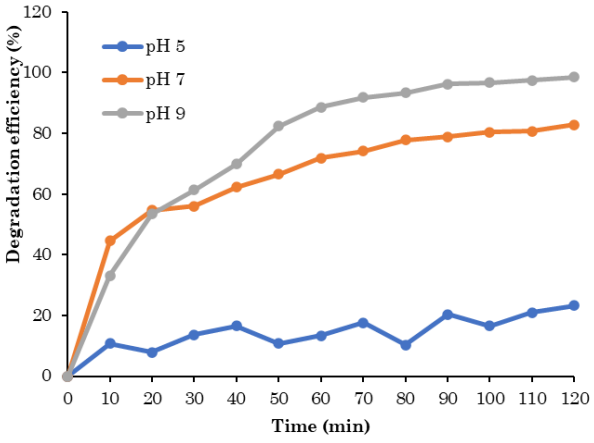

Figure 9. Effect of pH on the degradation efficiency of methylene blue.

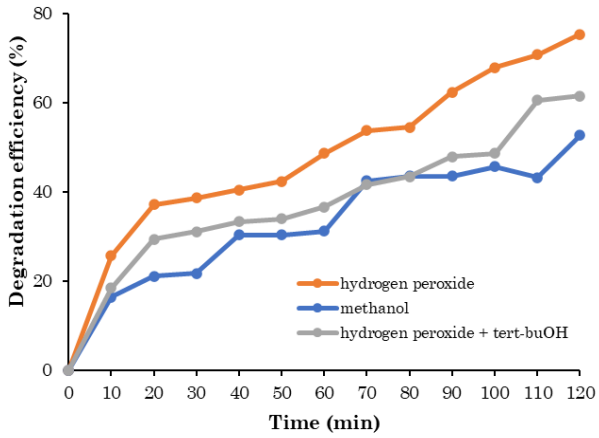

Figure 10. Effect of electron-hole scavenger on methylene blue degradation efficiency.

Copyright © 2023, ISSN 1978-2993

However, in this study it was found that the addition of H_2O_2 reduced the photocatalytic degradation efficiency of ZnO. Farrokhi *et al.* [30] explained that degradation efficiency can decrease due to the concentration of H_2O_2 used exceeding the optimum concentration. The excess H_2O_2 captures •OH radicals to produce hydroperoxyl radicals that are less reactive (equation (12)). Zulys *et al*. [31] also reported that if the concentration of H_2O_2 is added excessively, this poisons the active site of the photocatalyst. The greater the concentration of H_2O_2 used, the more the surface-active site of the photocatalyst is damaged or inactivated.

$$H_2O_2 + \bullet OH \rightarrow H_2O + \bullet HO_2 \quad (12)$$

In addition, the decrease in methylene blue degradation efficiency is also caused by the hydroxyl radical at higher concentrations undergoing a dimerization reaction to H_2O_2 (equation (13)). Besides that the hydroperoxyl radical ($\bullet HO_2$) can react strongly with the hydroxyl radical (•OH) to produce oxygen and water (equation (14)) [32].

$$2\bullet OH \rightarrow H_2O_2 \quad (13)$$
$$\bullet HO_2 + \bullet OH \rightarrow O_2 + H_2O \quad (14)$$

The addition of methanol used as an electron-hole scavenger (h^+) obtained a lower degradation efficiency than the addition of H_2O_2, which was 52.67%. It is due to the capture of electron-holes by methanol, causing no hydroxyl radicals (•OH) was formed and only superoxide radicals ($\bullet O_2$) present. The electron-holes (h^+) in the conduction band oxidize methanol to hydroxyalkyl radicals ($\bullet CH_2OH$) and are oxidized to formaldehyde (CH_2O), and prevent the formation of hydroxyl radicals. However, photoexcited electrons react with oxygen to form superoxide radicals ($\bullet O_2$). This superoxide radical($\bullet O_2$) plays a dominant role in this degradation process (Equations (15) and (16)) [31].

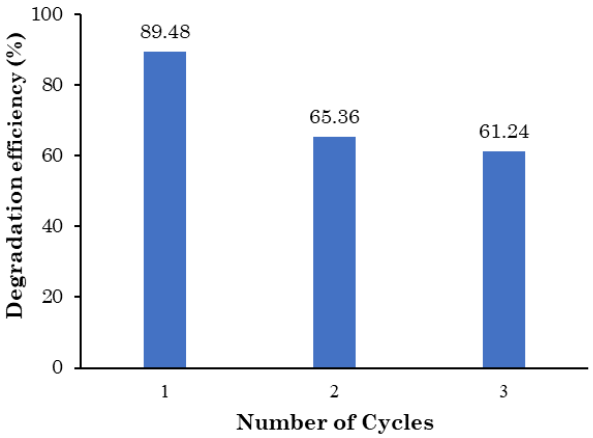

Figure 11. Reusability of ZnO nanoparticles.

$$h^+_{vb} + CH_3OH \rightarrow \bullet CH_2OH \quad (15)$$
$$CH_2OH \rightarrow CH_2O + H^+ + e^- \quad (16)$$

Adding a mixture of H_2O_2 and tert-butanol ($(CH_3)_3COH$) was carried out to reconfirm the dominant species playing a role in the degradation of methylene blue. Adding H_2O_2 and tert-butanol resulted in a degradation efficiency of 61.50%. It indicates that the addition of tert-butanol causes a decrease in degradation efficiency than the addition of H_2O_2 because tert-butanol captures the hydroxyl radical species (•OH) in the system and result in a lowering in the number of hydroxyl radicals, which play an important role in the methylene blue degradation process [31].

3.11 Reusability of ZnO Nanoparticles

The reusability and stability of ZnO nanoparticles analysis were conducted at a photocatalyst dosage of 75 mg, methylene blue concentration of 25 ppm, and a pH of 9 for 3 cycles. Separation of the ZnO nanoparticles after the reaction was carried out by washing the ZnO nanoparticles to remove residual methylene blue attached to the surface of the ZnO nanoparticles. Then the ZnO nanoparticles were dried at 80 °C for 2 h. The dried ZnO nanoparticles were reused for the next reaction cycle.

Figure 11 showed that the ZnO photocatalyst could be used for 3 cycles with 89.48%, 65.36%, and 61.24% degradation efficiencies. Figure 11 shows a decrease in degradation efficiency after 3 cycles to 61.24%. However, the results of this study were much better than previous studies, which produced ZnO nanoparticles with a degradation efficiency of 31.40% after 3 reaction cycles [33]. Marsel *et al.* [34] explained that the decrease in the photocatalytic activity of ZnO nanoparticles was due to reduced photocatalyst mass during the washing and drying processes, resulting in a smaller photocatalyst mass for the next cycle. Covering the pores and active sites on the catalyst's surface by dye molecules attached to the photocatalyst surface drives the photocatalyst inactive. It generates for lowering the photocatalytic activity of ZnO nanoparticles [34,35].

Meanwhile, the stability of ZnO nanoparticles after use in 3 reaction cycles was determined from the XRD analysis of ZnO nanoparticles, which can be seen in Figure 12. The Figure 12 shows no difference between the ZnO nanoparticle XRD diffractogram pattern before

Copyright © 2023, ISSN 1978-2993

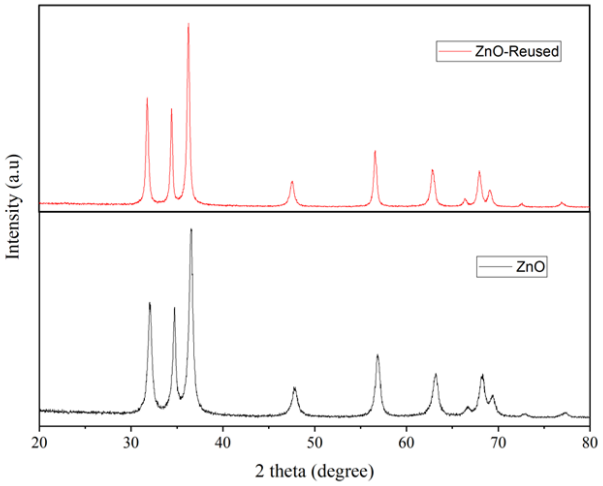

Figure 12. XD spectrum of ZnO nanoparticle before and after methylene blue photodegradation.

and after the reaction. It indicates that the ZnO nanoparticles have good stability for 3 cycles.

4. Conclusions

Morphology of synthesized ZnO nanoparticles is spherical, with a band gap energy of 3.21 eV, the particle size is 79.153 nm, and the crystal size is 19.324 nm. The ZnO nanoparticles have photodegradation activity against methylene blue with a degradation efficiency of 98.50% at 25 ppm methylene blue, and a mass of ZnO is 0.075% (w/v) at pH 9. The dominant species affecting methylene blue degradation are holes (h^+) and hydroxyl radicals (•OH). ZnO nanoparticles have good stability as a photocatalyst in degrading methylene blue under mercury lamp irradiation as an ultraviolet (UV) light source after three cycles.

Acknowledgment

The authors would like to thank UIN Syarif Hidayatullah Jakarta for financially supporting to carry out this research with the contract number B-302/LP2M-PUSLITPEN/TL.02/2023.

CRediT Author Statement

N. Saridewi was responsible for conceptualization, validation, and financial resources; S. Rustanti was on duty for formal analysis, investigation, and data gathering. A. Zulys and S. Nurbayti discussed research and resources. I. Aziz oversaw writing, reviewing, and editing. A. Adawiah was responsible for writing the manuscript. All authors read the manuscript and promptly approved it for future publication.

References

[1] Koyuncu, H., Kul, A.R. (2020). Removal of methylene blue dye from aqueous solution by nonliving lichen (*Pseudevernia furfuracea* (L.) Zopf.), as a novel biosorbent. *Applied Water Science*, 10, 72. DOI: 10.1007/s13201-020-1156-9.

[2] Sahu, S., Pahi, J. K., Sahu, U. K., Patel. (2020). Kendu (*Diospyros melanoxylon Roxb*) fruit peel activated carbon an efficient bioadsorbent for methylene blue dye: Equilibrium, kinetic, and thermodynamic study. *Environ. Sci. Pollut. Res*, 27, 22579–22592. DOI: 10.1007/s11356-020-08561-2.

[3] Khan, I., Saeed, K., Zekker, I., Zhang, B., Hendi, A., Ahmad, A. (2022). Review on Methylene Blue: Its Properties, Uses, Toxicity and Photodegradation. *Water*, 14(2), 242. DOI: 10.5040/9781501365072.12105.

[4] Kumar, P. S., Ramalingam, S., Sathishkumar, K. (2011). Removal of methylene blue dye from aqueous solution by activated carbon prepared from cashew nut shell as a new low-cost adsorbent. *Korean Journal of chemical engineering*, 28, 149-155. DOI: 10.1007/s11814-010-0342-0.

[5] Akbari, Z., Sabouri, Z., Hosseini, H. A, Hashemzadeh, A., Khatami, M., Darroudi, M. (2020). Effect of nickel oxide nanoparticles as a photocatalyst in dyes degradation and evaluation of effective parameters in their removal from aqueous environments. *Inorganic Chemistry Communications,* 115, 107867. DOI: 10.1016/j.inoche.2020.107867.

[6] Aliah, H., Karlina, Y. (2015). Semikonduktor TiO_2 sebagai material fotokatalis berulang. *Jurnal Istek*, 9(1), 185–203. ISSN 1979-8911

[7] Hassani, A., Farajia, M., Eghbali, P. (2020). Facile fabrication of mpg-C_3N_4/Ag/ZnO nanowires/Zn photocatalyst plates for photodegradation of dye pollutant. *Journal of Photochemistry & Photobiology A: Chemistry*, 400(2020), 112665. DOI: 10.1016/j.jphotochem.2020.112665

[8] Hassani, A., Krishnan, S., Scaria, J., Eghbali, P., Nidheesh, P. V. (2021). Z-scheme photocatalysts for visible-light-driven pollutants degradation: A review on recent advancements. *Current Opinion in Solid State and Materials Science,* 25 (2021) 100941. DOI: 10.1016/j.cossms.2021.100941.

[9] Samanta, P. K., Saha, A., Kamilya, T. (2015). Morphological and optical property of spherical ZnO nanoparticles. *Optik*, 126(18), 1740–1743. DOI: 10.1016/j.ijleo.2015.04.025.

Copyright © 2023, ISSN 1978-2993

[10] Ningsih, S. K. (2017). Sintesis dan karakterisasi nanopartikel ZnO doped Cu^{2+} melalui metoda sol-gel. *EKSAKTA: Berkala Ilmiah Bidang MIPA*, 18(02), 39-51. DOI: 10.1088/1751-8113/44/8/085201.

[11] Saridewi, N., Syaputro., Aziz, I., Dasumiati, D., Kumila. (2021). Synthesis and characterization of ZnO nanoparticles using pumpkin seed extract (*Cucurbita moschiata*) by the sol-gel method. *AIP Conference Proceedings* (Vol. 2349, No. 1). DOI: 10.1063/5.0051826.

[12] Sari, R. N., Nurhasni., Yaqin, M. A. (2017). Green Synthesis nanoparticle ZnO *Sargassum sp*. extract and the products charactheristic. *Jurnal Pengolahan Hasil Perikanan Indonesia*, 20(2), 238-254. DOI: 10.17844/jphpi.v20i2.17905.

[13] Dewatisari, W. F., Rumiyanti, L., Rakhmawati, I. (2018). Rendemen dan skrining fitokimia pada ekstrak daun *Sanseviera* sp. *Jurnal Penelitian Pertanian Terapan*, 17(3), 197-202. doi: 10.25181/jppt.v17i3.336.

[14] Makuła, P., Pacia, M., Macyk, W. (2017). How to correctly determine the band gap energy of modified semiconductor photocatalysts based on UV–Vis spectra. *The Journal of Physical Chemistry Letters,* 9(23)*, 6814-6817*. DOI: 10.1021/acs.jpclett.8b02892.

[15] Ifeanyichukwu, U. L., Fayemi, O. E., Ateba, C. N. (2020). Green synthesis of zinc oxide nanoparticles from pomegranate (*Punica granatum*) extracts and characterization of their antibacterial activity. *Molecules*, 25(19), 4521.DOI: 10.3390/molecules25194521.

[16] Marslin, *G*., Siram, K., Maqbool, Q., Selvakesavan, R., Kruszka, D., Kachlicki, P., Franklin, G. (2018). Secondary metabolites in the green synthesis of metallic nanoparticles. *Materials,* 11(6), 940. DOI: 10.3390/ma11060940.

[17] Tournebize, J., Boudier, O., Joubert, H., Eidi, G., Bartosz, P., Maincent, P., Leroy, Sapin. (2012). Impact of gold nanoparticle coating on redox homeostasis. *International Journal of Pharmaceutics*, 438(1-2), 107-116. DOI: 10.1016/j.ijpharm.2012.07.026.

[18] Ajmal, A. W., Masood, F., Yasin, T. (2018). Influence of sepiolite on thermal, mechanical and biodegradation properties of poly-3-hydroxybutyrate-co-3-hydroxyvalerate nanocomposites. *Applied Clay Science*, 156, 11-19. DOI: 10.1016/j.clay.2018.01.010.

[19] Nurbayasari, R., Saridewi, N., Shofwatunnisa. (2017). Biosynthesis and characterization of ZnO nanoparticles with extract of green seaweed *Caulerpa* sp. *Jurnal Perikanan Universitas Gadjah Mada*, 19(1), 17-28. DOI: 10.22146/jfs.24488.

[20] Soto-Robles, C. A., Nava, O., Cornejo, L. (2021). Biosynthesis, characterization and photocatalytic activity of ZnO nanoparticles using extracts of Justicia spicigera for the degradation of methylene blue. J*ournal of Molecular Structure*, 1225, 129101. DOI: 10.1016/j.molstruc.2020.129101.

[21] Sangeetha, G., Rajeshwari, S., Venckatesh, R. (2011). Green synthesis of zinc oxide nanoparticles by aloe barbadensis miller leaf extract: Structure and optical properties. *Materials Research Bulletin*, 46(12), 2560-2566. DOI: 10.1016/j.materresbull.2011.07.046.

[22] Vasquez, R. D., Apostol, J. G., de Leon, J. D., Mariano, J. D. (2016). Polysaccharide-mediated green synthesis of silver nanoparticles from Sargassum siliquosum JG Agardh: assessment of toxicity and hepatoprotective activity. *OpenNano*, 1, 16-24. DOI: 10.1016/j.onano.2016.03.001.

[23] Alshehri, A., Malik, A. (2019). Biogenic fabrication of ZnO nanoparticles using *Trigonella foenum-graecum* (Fenugreek) for proficient photocatalytic degradation of methylene blue under UV irradiation. *Journal of Materials Science: Materials in Electronics*, 30, 16156-16173. DOI: 10.1007/s10854-019-01985-8.

[24] Balcha, A., Yadav, O. P., Dey. (2016). Photocatalytic degradation of methylene blue dye by zinc oxide nanoparticles obtained from precipitation and sol-gel methods. *Environmental Science and Pollution Research*, 23, 25485-25493. DOI: 10.1007/s11356-016-7750-6.

[25] Chiu, Y. H., Chang., Chen, C. Y., Sone, M., Hsu, Y. J. (2019). Mechanistic insights into photodegradation of organic dyes using heterostructure photocatalysts. *Catalysts*, 9(5), 430. DOI: 10.3390/catal9050430.

[26] Kumar, A. (2017). A Review on the Factors Affecting the Photocatalytic Degradation of Hazardous Materials. *Mater. Sci. Eng. Int. J.*, 1(3), 106–114. DOI: 10.15406/mseij.2017.01.00018.

[27] Riskiani, E., Suprihatin, I. E., Sibarani, J. (2018). Fotokatalis bentonit-Fe_2O_3 untuk Degradation zat warna remazol brilliant blue. *Cakra Kimia (Indonesian E-Journal of Applied Chemistry)*, 7(1).

[28] Jeon, Y. H., Kwon, J. J., Lee, B. H. (2006). Study on pH sensor using methylene blue adsorption and a long-period optical fiber grating pair. *Journal of the Optical Society of Korea*, 10(1), 28-32. DOI: 10.3807/josk.2006.10.1.028

[29] Lee, K. M., Lai, C. W., Ngai, K. S., Juan, J. C. (2015). Recent developments of zinc oxide based photocatalyst in water treatment technology: A review, *Water Research*, 88, 428-448. DOI: 10.1016/j.watres.2015.09.045.

Copyright © 2023, ISSN 1978-2993

[30] Farrokhi, A., Jafarpour, M., Alipour, M. (2019). Solar-driven advanced oxidation process catalyzed by metal–organic frameworks for water depollution. *Polyhedron*, 170, 325–333. DOI: 10.1016/j.poly.2019.06.005.

[31] Zulys, A., Adawiah, Gunlazuardi, J., Yudhi. (2021). Light-harvesting metal-organic frameworks (MOFs) La-PTC for photocatalytic dyes degradation. *Bulletin of Chemical Reaction Engineering & Catalysis*, 16(1), 170-178. DOI: 10.9767/bcrec.16.1.10309.170-178.

[32] Abramovic, B., Despotovic, V., Šojic, D., Fincur, N. (2015). Mechanism of clomazone photocatalytic degradation: hydroxyl radical, electron and hole scavengers. *Reaction Kinetics, Mechanisms and Catalysis*, 115, 67-79. DOI: 10.1007/s11144-014-0814-z.

[33] Kitture, R., Koppikar, S. J., Kaul-Ghanekar, R., Kale, S. N. (2011). Catalyst efficiency, photostability and reusability study of ZnO nanoparticles in visible light for dye degradation. *Journal of Physics and Chemistry of Solids*, 72(1), 60-66. DOI: 10.1016/j.jpcs.2010.10.090.

[34] Marsel, N., Imani, T., Kato, D., Oshima, E. (2022). High reusability of greensynthesized Fe_3O_4/TiO_2 photocatalyst nanoparticles for efficient degradation of methylene blue dye. *Materials Today Communications*, 33, 104450. DOI: 10.1016/j.mtcomm.2022.104450.

[35] Sin, J. C., Lam, S. M., Zeng, H., Lin, H., Li, H., Huang, L., Lim, J. W. (2022). Enhanced synchronous photocatalytic 4-chlorophenol degradation and Cr (VI) reduction by novel magnetic separable visible-light-driven Z-scheme $CoFe_2O_4$/P-doped BiOBr heterojunction nanocomposites. *Environmental Research*, 212, 113394. DOI: 10.1016/j.envres.2022.113394.

Copyright © 2023, ISSN 1978-2993